Sinklike spiral waves in oscillatory media with a disk-shaped inhomogeneity

Bing-Wei Li,[1] Hong Zhang,[1,*] He-Ping Ying,[1] Wen-Qiang Chen,[1] and Gang Hu[2]
[1]*Zhejiang Institute of Modern Physics and Department of Physics, Zhejiang University, Hangzhou 310027, China*
[2]*Department of Physics and the Beijing–Hong Kong–Singapore Joint Centre for Nonlinear and Complex Systems (Beijing), Beijing Normal University, Beijing 100875, China*

(Received 13 May 2007; revised manuscript received 27 January 2008; published 15 May 2008)

Spiral wave propagation in oscillatory media with a disk-shaped inhomogeneity is examined. Depending on the properties of the medium as well as the inhomogeneity (different frequencies in two regions), distinct spiral waves including sinklike spirals and dense-sparse spirals, are able to emerge. We find that, unlike the previously found outward group velocity for spiral waves (normal spirals or antispirals), the direction of the velocity of the sinklike spiral wave points inward. A qualitative analysis of the possible mechanism underlying their formation is discussed, considering the inhomogeneity as a wave sink or source. Numerical simulations performed on other typical reaction-diffusion models confirm this analysis and suggest that our findings are robust and could be observed in experiments.

DOI: 10.1103/PhysRevE.77.056207 PACS number(s): 89.75.Kd, 47.54.−r, 82.40.Ck

I. INTRODUCTION

Pattern formation and wave propagation in chemical systems have been investigated extensively because of their potential roles in the understanding of morphogenesis and functional aspects in biological systems [1,2]. As is well known, spiral waves found in chemical systems, e.g., the Belousov-Zhabotinsky (BZ) reaction [3–5] and catalytic surface reactions [6], are relevant for biological functions including aggregation of the social amoeba *Distyostelium discoideum* [7] as well as some serious arrhythmias taking place in heart tissue [8–11]. From this point of view, understanding spiral dynamics may have potential practical applications that hence have inspired numerous studies in last decades.

While so far most work has focused on wave dynamics in homogeneous active media, nonlinear systems with inhomogeneous media actually offer an attractive subject for investigation due to their common occurrence and importance. In biological media such as heart tissue, there exist defective regions (e.g., disease cells due to myocardial infarction) which make the medium nonuniform [12–14]; impurities (e.g., dust particles, gas bubbles, etc.) and temperature fluctuations are regarded as sources of reaction rate inhomogeneity in practical reaction-diffusion (RD) systems [15,16]. In some situations the inhomogeneity could play an important role in pattern-forming systems. For instance, the presence of a heterogeneity, which locally modifies the properties of the medium, is able to induce an extended target pattern [17–22]; antispirals have been found in the microheterogeneous BZ system dispersed in water droplets of a water-in-oil microemulsion [5] and in assemblies of oscillatory cells consisting of the active intracellular medium separated by inactive extracellular parts [23]; sink-source pairs of spiral waves are observed experimentally on spherical surfaces possibly with inhomogeneous chemical environments [24] and in numerical simulations if the excitability gradient is applied [25].

In this paper, we will analyze the spiral dynamics in oscillatory systems with a disk-shaped inhomogeneity. Much attention has been paid to wave propagation as well as the interaction of spiral waves in composite media with a line interface [26–33]; the effects of other geometries such as sharp triangles or ring shapes on chemical wave propagation are also studied in Refs. [34,35]. Yet little is known about the spiral behavior in heterogeneous media consisting of an interior region surrounded by an exterior region with different properties, i.e., the bulk frequency. In this circumstance, we will show that distinct spiral patterns can arise and their formation greatly depends on the properties of the medium as well as the inhomogeneity. We notice that one of the spiral patterns formed, named sinklike spiral waves, quite differs from the previously found spirals such as normal spirals (NSs) and antispirals (ASs). For NSs and ASs, the group velocity always points outward, while for the sinklike spiral it points inward. Based on the view of the inhomogeneity being a wave source or sink, we address the possible mechanism underlying the formation of sinklike spiral patterns and related features. Further simulations performed on other RD models indicate that the results presented here are robust.

II. SINKLIKE SPIRAL WAVES IN THE COMPLEX GINZBURG-LANDAU EQUATION

A general RD system in two dimensions (2D) can be described by a set of partial differential equations as

$$\frac{\partial \mathbf{u}}{\partial t} = \mathbf{F}(\mathbf{u}, \mu) + \mathbf{D}\nabla^2 \mathbf{u}, \tag{1}$$

where $\mathbf{u}(\mathbf{x},t)$ is a space- and time-dependent vector describing the various chemical species; $\mathbf{F}$ is a kind of nonlinear vectorial function representing the chemical kinetics; $\mathbf{D}$ generally is a diagonalized diffusion matrix, and μ is a control parameter. Close to the supercritical Hopf bifurcation, RD systems can be reduced to the simple complex Ginzburg-Landau equation (CGLE) [18,37–39],

*Author to whom correspondence should be addressed. hzhang@zimp.zju.edu.cn

$$\frac{\partial W}{\partial t} = (1 - i\omega)W - (1 + i\alpha)|W|^2 W + (1 + i\beta)\nabla^2 W, \quad (2)$$

where $W(x,y,t)$ is a complex variable describing the amplitude of the pattern modulations. The parameters α and β are real, representing the nonlinear frequency shift and dissipative coefficient, respectively. ω describes the linear frequency and $\nabla^2 = \partial^2/\partial x^2 + \partial^2/\partial y^2$ denotes the 2D Laplacian operator. Equation (2) admits a stable spiral solution, which can be written in polar coordinates as [40]

$$W(r,\theta,t) = \rho(r)e^{i\phi} = \rho(r)e^{i[-\Omega_k t + \sigma\theta + \psi(r)]}, \quad (3)$$

where $\sigma = \pm 1$ is the "topological charge" of the one-arm spiral wave. $\rho(r)$ and $\psi(r)$ are real functions, which have the following asymptotic behavior far from the center: $d\psi/dr \to k$ and $\rho \to \sqrt{1-k^2}$ as $r \to \infty$. Hence, for large r, the spiral solution (3) asymptotes to the plane wave solution,

$$W(\mathbf{r},t) = \sqrt{1-k^2}e^{i(-\Omega_k t + \mathbf{k}\cdot\mathbf{r})}. \quad (4)$$

Here, the asymptotic frequency Ω_k and wave number k are related via the nonlinear dispersion relation

$$\Omega_k = \Omega_0 + (\beta - \alpha)k^2, \quad (5)$$

where $\Omega_0 = \omega + \alpha$ is the bulk frequency (i.e., the frequency of uniform oscillation of the system with $k=0$) and $\beta - \alpha > 0$ ($\beta - \alpha < 0$) represents the positive (negative) dispersion curve. From Eq. (5), the group velocity and phase velocity can be derived analytically as

$$v_{\mathrm{gr}} = \frac{d\Omega_k}{dk} = 2(\beta - \alpha)k, \quad (6)$$

$$v_{\mathrm{ph}} = \frac{\Omega_k}{k} = \frac{\Omega_0}{k} + (\beta - \alpha)k. \quad (7)$$

The sign of v_{gr} physically determines the direction in which perturbations are transported, away from or toward the center of the wave patterns. To some extent, it also correlates with an organizing center if the direction of the group velocity is outward. From this point, the centers of NSs ($v_{\mathrm{ph}} > 0$) and ASs ($v_{\mathrm{ph}} < 0$) are both organizing centers since $v_{\mathrm{gr}} > 0$ always holds for both cases [41–45].

To address spiral behavior in composite oscillatory media, we consider ω as a spatial function,

$$\omega(r) = \begin{cases} 0 & \text{for } r > R, \\ \Delta\omega & \text{for } r \le R, \end{cases} \quad (8)$$

where $r = \sqrt{(x-x_c)^2 + (y-y_c)^2}$ and (x_c, y_c) denotes the center of the studied medium. The radius R of the center region (core region) considered here is comparable to the scale of the medium. Strictly speaking, our numerical results depend on the value of R; but this dependence is slight if R is beyond the critical value R_c, which is relatively small compared to the scale of the whole medium. The effects induced by a localized inhomogeneity (R is quite small) have been investigated in our recent paper [21] and thus only the case of large R will be considered in this paper. It is noticed that the change of ω is essentially equal to modulation of the bulk frequency since $\Omega_0 = \omega + \alpha$. In our numerical simulations of the CGLE, the space and time steps are $\Delta x = \Delta y = 1.0$ and $\Delta t = 0.5$, respectively. No-flux conditions are imposed at the boundaries. The initial condition we used is a well-developed spiral generated from a cross-gradient initial condition for Re W and Im W [18].

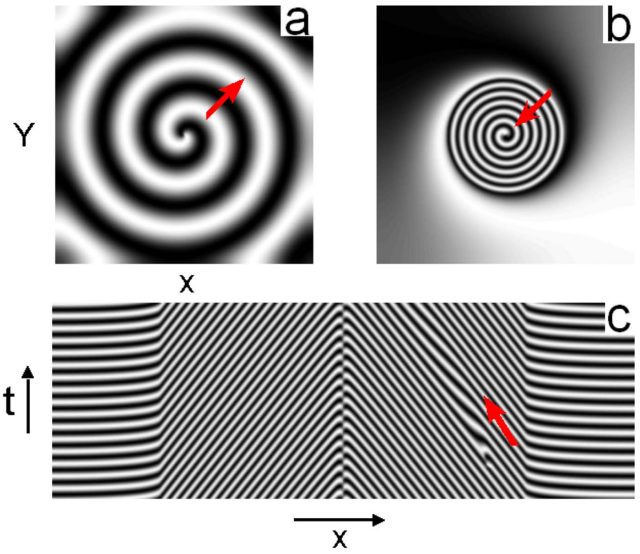

FIG. 1. (Color online) Sinklike spiral in CGLE (2) with the parameters $\alpha = -0.5$ and $\beta = -1.4$. (a) Initial condition, $\Delta\omega = 0$. (b) Sinklike spiral waves, $\Delta\omega = 0.2$, radius $R = 90$, 400×400 system; the red arrow denotes the direction of the group velocity. (c) Space-time plot along a horizontal cut at $y = 400$ for a sinklike spiral, radius $R = 250$, 800×800 system; the red arrow denotes the direction in which the artificial perturbation is transported. The plots are shown for the CGLE in the real part of W. The space and time steps are $\Delta x = \Delta y = 1.0$ and $\Delta t = 0.5$, respectively. No-flux conditions are imposed at the boundaries.

When $\Delta\omega = 0$, the difference between the two regions vanishes and hence the medium recovers homogeneity. In this case, whether NSs or ASs will emerge from the same initial condition is determined uniquely by two parameters α and β. According to the phase portrait presented in Refs. [41,42], with the parameters $\alpha = -0.5$ and $\beta = -1.4$, a cross-gradient initial value of Re W and Im W will lead to a well-developed NS whose phase singularity ($|W| = 0$) is located at the center of the medium [see Fig. 1(a)]. A remarkable change of spiral behavior takes place when an inhomogeneity is introduced in the center region, e.g., $\Delta\omega = 0.2$, still with $\alpha = -0.5$ and $\beta = -1.4$ throughout the medium. After a transient time, a new kind of spiral waves is formed eventually as illustrated in Fig. 1(b). The newly arising features compared to the initial spiral [Fig. 1(a)] are characterized briefly as follows. The first point, maybe the most interesting feature, is the inward (or negative) group velocity of the newly formed spiral waves. A detailed discussion about this feature is presented below. Second, the phase velocity v_{ph} is changed. For the initial NS ($v_{\mathrm{ph}} > 0$), periodic waves propagate from the spiral center to the periphery, while now there is an exactly contrasting case where waves begin to propagate from the periphery to the sinklike spiral center as illustrated in the space-time plot [see Fig. 1(c)]. Third, the difference of the wave number k in the two regions is apparent. As shown in Figs.

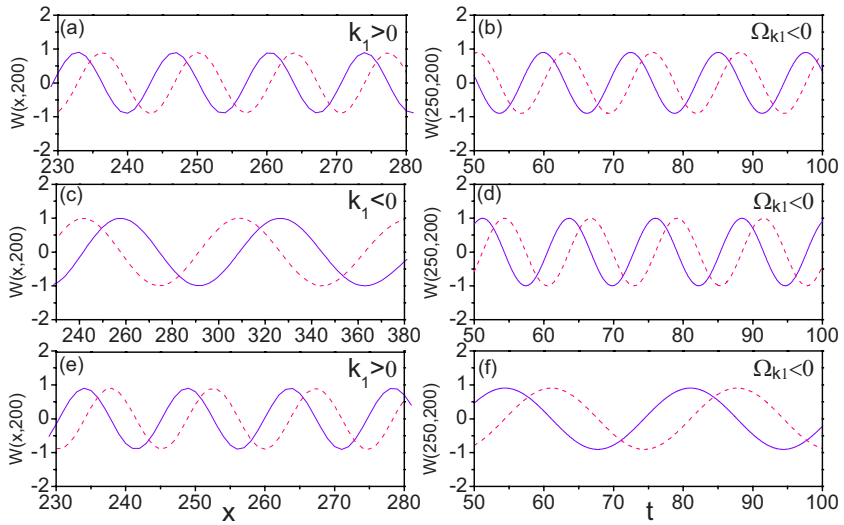

FIG. 2. (Color online) Profile of Re W (solid line) and Im W (dashed line) vs time (t) and space (x) for three different spiral patterns. (a),(b) Sinklike spiral waves with parameters $\Delta\omega=0.2$, $\alpha=-0.5$, and $\beta=-1.4$; $\beta-\alpha<0$. From (a) and with Eq. (4), we find $k_1>0$. Similarly, according to (b) and with Eq. (4), we get $\Omega_{k_1}<0$. Using Eqs. (6) and (7), we finally get $v_{\rm ph}<0$ and $v_{\rm gr}<0$. This conclusion reveals that the sinklike spiral pattern is an unusual one because it differs from previously found spirals such as NSs or ASs, whose group velocity is always positive, $v_{\rm gr}>0$ (see below). (c),(d) NS with the parameters $\Delta\omega=0.0$, $\alpha=-0.5$, and $\beta=-1.4$; $\beta-\alpha<0$. With the same arguments as above, we get $k_1<0$ and $\Omega_{k_1}<0$, which results in $v_{\rm ph}>0$ and $v_{\rm gr}>0$. (e),(f) AS with the parameters $\Delta\omega=0.0$, $\alpha=-0.5$, and $\beta=1.0$; $\beta-\alpha>0$. Analogously, we find $k_1>0$ and $\Omega_{k_1}<0$. This means for the AS $v_{\rm ph}<0$ and $v_{\rm gr}>0$. This gives evidence that these simple arguments for NSs and ASs lead to the same results obtained by other methods [41,44]. x here is the horizontal axis cut at $y=200$ and its origin is located at the spiral tip (200, 200) in the present case. Therefore, the positive x direction is to the right of the origin, i.e., $x>200$.

1(b) and 1(c), the spiral arms in the core region look much denser than the ones in the outside region.

We would like to emphasize that the group velocity of the newly formed spiral pattern is inward, unlike previously found spiral waves (either NS or AS) whose group velocity points outward. To show this point, a standard procedure to determine the group velocity of waves as well as a qualitative analysis are performed for the CGLE. We first employ the standard procedure, simulating the transport of a small perturbation superimposed on the sinklike spiral pattern, to find the direction of the group velocity. To show this more clearly, we do this simulation on a much larger system, i.e., 800×800 grid points with $R=250$. As indicated by the red arrow in Fig. 1(c), the small perturbation artificially introduced is found to be transported toward the center of the newly formed spiral pattern. For this reason, we call it a sinklike spiral wave. Alternatively, from Eq. (6) or Eq. (7), we find that, to determine the sign of the group or phase velocity, it is beneficial to know the sign of the wave number k and the frequency Ω_k. As Eq. (4) indicates, the sign of these two quantities can be found if we know whether Im W is ahead of or behind Re W. Explicitly, for a snapshot of Im W and Re W at any time [for example, Figs. 2(a), 2(c), and 2(e)], it is straightforward to show that Im W is behind Re W, implying $k<0$, and vice versa; similarly for the motion of a single point for Im W and Re W [for instance, Figs. 2(b), 2(d), and 2(f)], Im W is behind Re W, implying $\Omega_k<0$, and vice versa. Note that in a plot of Im W or Re W versus x, "ahead of" means "to the right of" if the waves travel in the positive x direction (in our case "the positive x direction" means to the right of the tip location along the horizontal line, i.e., $x>200$); whereas in a plot of Im W or Re W versus t "ahead of" means "to the left of." Thus, it is easy to find the signs of the group and phase velocities for the plots shown in Fig. 2. For the sinklike spiral wave, we can see from Fig. 2(a) that Im W is ahead of Re W, indicating $k_1>0$ (k_1 represents the wave number in the inner region); similarly from Fig. 2(b) we find that Im W is behind Re W meaning $\Omega_{k1}<0$. Consequently, we finally get $v_{\rm gr}=d\Omega_{k1}/dk_1=2k_1(\beta-\alpha)<0$ since $(\beta-\alpha)<0$ and $v_{\rm ph}=\Omega_{k1}/k_1<0$ in this case, which is in agreement with the result shown in Fig. 1(c). As we expect, this simple argument can also be applied to NSs [see Figs. 2(c) and 2(d)] and ASs [see Figs. 2(e) and 2(f)]. The above conclusion reveals that the sinklike spiral pattern is an unusual one because it differs from previously found spirals such as NSs or ASs, whose group velocity is always positive, $v_{\rm gr}>0$. One may notice that this feature is similar to the concave spiral found in excitable media with parameters in the solitonlike region [46]. The formation of concave spirals in excitable media is a result of reflection of slave waves and thus depends strongly on the boundary conditions; while the resulting sinklike spiral is induced by inhomogeneity in the oscillatory media. Therefore, they are not the same case.

Whether a sinklike spiral is formed or not is determined by properties of the medium (β,α) as well as the inhomogeneity $(\Delta\omega)$. To demonstrate this point, we further perform the following numerical tests. As a first case, we still keep $\alpha=-0.5$ and $\beta=-1.4$ but change the sign of $\Delta\omega$, i.e., $\Delta\omega=-0.2$, and in this case $(\beta-\alpha)\Delta\omega>0$. We find that a different kind of spiral pattern, called dense-sparse spiral waves, differing from the sinklike spiral appears [see Fig. 3(a)]. Unlike the case $\Delta\omega=0.2$, where $(\beta-\alpha)\Delta\omega<0$, the change of spiral in this case is more gradual. Although we just change

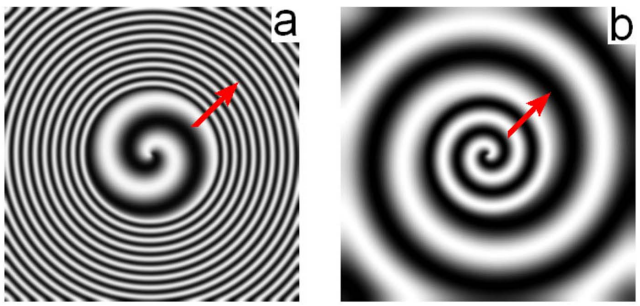

FIG. 3. (Color online) Two other distinct spiral patterns mediated by the inhomogeneity: (a) dense-sparse spiral waves, $\Delta\omega=-0.2$, $\alpha=-0.5$, and $\beta=-1.4$; (b) sparse-dense spiral waves, $\Delta\omega=-0.02$, $\alpha=0.3$, and $\beta=1.4$. The red arrow denotes the direction of the group velocity. The other parameters are chosen the same as Fig. 1.

the bulk frequency in the center region, the change of the pattern there is small. In contrast, the change of the spiral pattern in the outside region where the parameters are kept the same as the initial ones, is considerable. To be precise, the spiral arms in the outside region become denser compared with the ones in the center region. In the second test, we modify the properties of the medium. For instance, we adopt $\alpha=0.3$ and $\beta=1.4$ satisfying $\beta-\alpha>0$. In this situation, we find that the oscillation bulk frequency in the center region should be decreased, namely, $\Delta\omega<0$, if a sinklike spiral is able to emerge. One may note that in this case $(\beta-\alpha)\Delta\omega<0$ still holds. However, this condition $[(\beta-\alpha)\Delta\omega<0]$ is not sufficient to generate sinklike spiral patterns unless $\Delta\omega$ is not too small. For $(\beta-\alpha)\Delta\omega<0$, but with a too small $\Delta\omega$, another kind of wave pattern (sparse-dense spiral waves) is generated and in this case the spiral arms in the center region are denser than the ones in the outside region, as shown in Fig. 3(b). This feature is in contrast to the dense-sparse case. Thus to form the sinklike spiral, in addition to $(\beta-\alpha)\Delta\omega<0$, $\Delta\omega$ should be over a critical value that depends on the system parameters (α,β).

To give a clearer picture, we propose the phase diagram of the types of solution in the $(\beta-\alpha)$ vs $\Delta\omega$ plane for the CGLE system in Fig. 4. One finds that the results shown in the phase diagram are in agreement with the above statements. Explicitly, sinklike as well as sparse-dense spiral waves are observed in the regions in which $(\beta-\alpha)\Delta\omega<0$ is satisfied; whereas dense-sparse spiral waves are observed in the regions where $(\beta-\alpha)\Delta\omega>0$ holds. In addition to these kinds of waves, other complicated wave patterns, for instance wave breaks, wave blocks at the interface, etc., are also found.

In Fig. 5, we show the dependence of the frequency Ω_{k1} and absolute wave number $|k_1|$ in the center region on $\Delta\omega$ for two different cases: $\beta-\alpha<0$ and $\beta-\alpha>0$. For $\beta-\alpha<0$, we find that there is a linear dependence of Ω_{k1} on $\Delta\omega$ and a slight change of $|k_1|$ if we decrease $\Delta\omega$ for $\Delta\omega<0$ [see Figs. 5(a) and 5(b)]. This case corresponds to the dense-sparse spiral. In contrast, for $\Delta\omega>0$, Ω_{k1} has almost no change and $|k_1|$ depends linearly on $\Delta\omega$, which corresponds to the sinklike spiral. This kind of dependence is similar to the case for $\beta-\alpha>0$ [see Figs. 5(c) and 5(d)], but one should change the sign of $\Delta\omega$.

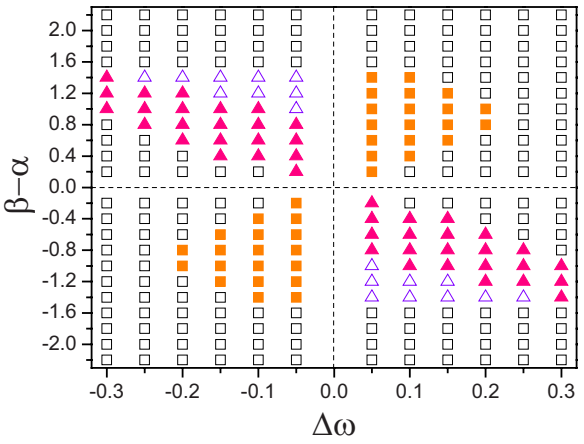

FIG. 4. (Color online) Phase diagram of the CGLE system for $(\beta-\alpha)$ vs $\Delta\omega$. Full triangles denote sinklike spiral waves and empty triangles represent sparse-dense spiral waves; while full squares denote dense-sparse spiral waves and empty squares represent other complicated wave patterns (for instance, wave breaks, wave blocks at the interface, etc.), which are beyond the scope of the present study. $\beta=0$ is kept constant and the initial condition of a cross-gradient value of Im W and Re W is employed to calculate this phase diagram.

III. SINKLIKE SPIRAL WAVES IN THE FITZHUGH-NAGUMO MODEL

Sinklike spiral waves are expected to be reproduced in oscillatory RD systems close to the supercritical Hopf bifurcation. Numerical simulations are carried out in the standard FitzHugh-Nagumo (FHN) model [47]

$$\frac{\partial u}{\partial t}=u-\frac{u^3}{3}+v+D_u\nabla^2 u$$

$$\frac{\partial v}{\partial t}=\epsilon(u-\gamma v+\eta)+D_v\nabla^2 v, \tag{9}$$

where $\epsilon>0$ is the ratio between the inhibitor variable v and active variable u. γ and η are two other control parameters that completely determine the number of fixed points $[u-u^3/3+v=0$ and $\epsilon(u-\gamma v+\eta)=0]$. For the sake of simplicity, we will consider only the case where a unique fixed point exists. For $0<\gamma<1$, we get the fixed point (u_{ss},v_{ss}) and a critical value $\epsilon_{hc}=(1-u_{ss}^2)/\gamma$. Linear stability analysis shows that, if the fixed point exhibits limit cycle behavior, the following condition should be met: $\epsilon<\epsilon_{hc}$. Following any one of Refs. [18,37,41], one can construct the relation between the parameters ω, α, and β in the CGLE and the parameters η, γ, and δ in the FHN model,

$$\omega=\frac{1-\gamma+\gamma u_{ss}^2}{\sqrt{\gamma(1-u_{ss}^2)-\gamma^2(1-u_{ss}^2)^2}}, \tag{10}$$

$$\alpha=\frac{3-3\gamma-7u_{ss}^2+3\gamma u_{ss}^4}{3\gamma+3\gamma u_{ss}^2-3}\sqrt{\frac{\gamma}{(1-u_{ss}^2)(1-\gamma+\gamma u_{ss}^2)}}, \tag{11}$$

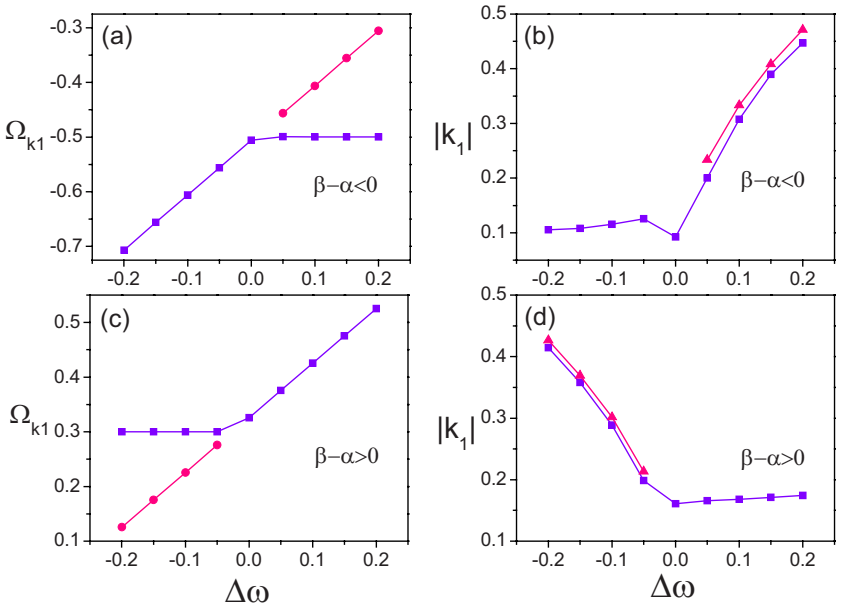

FIG. 5. (Color online) Dependence of frequency and wave number in the center region on $\Delta\omega$ for $\beta-\alpha<0$ and $\beta-\alpha>0$, respectively. (a) Dependence of frequency in center region on $\Delta\omega$ with the parameters $\alpha=-0.5$, $\beta=-1.4$, and $R=90$ for the squares and solid line and ∞ for the circle and solid line. (b) Dependence of wave number in center region on $\Delta\omega$. The parameters are the same as in (a) for the squares and solid line. The triangles and solid line describe the relation between wave number and $\Delta\omega$ via Eq. (24). (c) Similar to (a) but with different parameters $\alpha=0.3$, $\beta=1.4$, and $R=90$ for the squares and solid line and ∞ for the circles and solid line. (d) Similar to (b) but with the parameters as in (c) for the squares and solid line.

$$\beta = \frac{1-u_{ss}^2}{\sqrt{(1-u_{ss}^2)/\gamma-(1-u_{ss}^2)^2}}\frac{\delta-1}{\delta+1}, \tag{12}$$

where $\delta=D_v/D_u$, $u_{ss}=[(\sqrt{1+9\eta^2}-3\eta)^{2/3}-1]/(\sqrt{1+9\eta^2}-3\eta)^{1/3}$, and $v_{ss}=(u_{ss}+\eta)/\gamma$. For convenience, we take $\delta=1.0$ ($\beta=0.0$). To keep the parameter α constant in the whole medium and introduce only the variation reflected by ω for the FHN model, we rewrite γ and η as a spatial-dependent piecewise function in the following manner:

$$\gamma = \begin{cases} \gamma_2 & \text{for } r > R, \\ \gamma_1 & \text{for } r \le R, \end{cases} \tag{13}$$

and

$$\eta = \begin{cases} \eta_2 & \text{for } r > R, \\ \eta_1 & \text{for } r \le R. \end{cases} \tag{14}$$

Here γ_1, η_1, γ_2, and η_2 satisfy $\alpha(\gamma_1,\eta_1)=\alpha(\gamma_2,\eta_2)$ and the only change can be written as

$$\omega = \begin{cases} \omega_0 & \text{for } r > R, \\ \omega_0+\Delta\omega & \text{for } r \le R, \end{cases} \tag{15}$$

which is quite similar to the above case where we vary the parameter ω in the CGLE. As an example, we set $\gamma_1=0.2975$, $\eta_1=0.0$, $\gamma_2=0.30$, and $\eta_2=0.024$ and in this situation the corresponding α and $\Delta\omega$ are equal to -0.6507 and 0.0068, respectively. Figure 6(a) shows a sinklike spiral in the nonuniform FHN model with the above parameters. Keeping the same values of α and β, we find that dense-sparse spiral waves will emerge if we alter the sign of $\Delta\omega$, as shown in Fig. 6(b).

It should be pointed out that, for the FHN model, sinklike spiral waves could be observed if $(\beta-\alpha)\,\Delta\omega>0$ is satisfied. At first glance, this seems to contrast with the condition under which sinklike spiral waves emerge in the CGLE system; however, they are in principle coincident, which will be clear if we write out the bulk frequency for both systems explicitly. It has been shown that for the RD system the bulk frequency is as follows [41]:

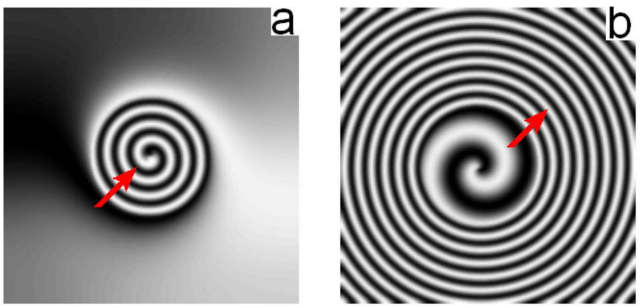

FIG. 6. (Color online) (a) Sinklike spiral pattern and (b) dense-sparse spiral waves in the nonuniform FHN model. (a) $(\gamma_1,\eta_1,\gamma_2,\eta_2)=(0.2975,0.0,0.300,0.024)$ and in this case $\Delta\omega=0.0068$. (b) $(\gamma_1,\eta_1,\gamma_2,\eta_2)=(0.300,0.024,0.2975,0.0)$ and in this case $\Delta\omega=-0.0068$. Other parameters are $\epsilon=3.31$, $D_u=D_v=0.005$, and $R=40$. The red arrow denotes the direction of the group velocity. Numerical simulations are carried out on 200×200 grid points employing the explicit Euler method. The space and time step are $\Delta x=\Delta y=0.5$ and $\Delta t=0.02$, respectively. No-flux conditions are imposed at the boundaries. The initial condition is a cross-gradient value of u and v.

$$f_{\text{bulk}}^{\text{RD}} = \Omega_{\text{Hopf}} - \frac{\varepsilon}{\tau}(\omega + \alpha), \tag{16}$$

where Ω_{Hopf} denotes the Hopf oscillation frequency for the RD system and ε/τ is a positive parameter. Equation (16) indicates that $\Delta f_{\text{bulk}}^{\text{RD}} \propto -\Delta\omega$, which is contrast to the case of the CGLE system where $\Delta f_{\text{bulk}}^{\text{CGLE}} \propto \Delta\omega$. Therefore, the inhomogeneity introduced by $\Delta\omega$ for the RD system (e.g., the FHN model) is regarded as a wave sink when $(\beta-\alpha)\Delta\omega > 0$ and a wave source when $(\beta-\alpha)\Delta\omega < 0$. This is the reason that we could observe sinklike spiral waves (dense-sparse spiral waves) if $(\beta-\alpha)\Delta\omega > 0$ $[(\beta-\alpha)\Delta\omega < 0]$ for the FHN system.

IV. THEORETICAL ANALYSIS

We so far have given a detailed discussion concerning the conditions under which sinklike spiral patterns could emerge; further questions including the possible mechanism of formation as well as the features formed may be addressed with theoretical considerations.

Substituting (3) into the CGLE (2), we get [18,21]

$$\frac{\partial \rho}{\partial t} = \rho - \rho^3 + \nabla^2\rho - \rho(\nabla\phi)^2 - \beta(2\,\nabla\rho\cdot\nabla\phi + \rho\nabla^2\phi), \tag{17}$$

$$\frac{\partial \phi}{\partial t} = -\omega(r) - \alpha\rho^2 + \nabla^2\phi - \beta(\nabla\phi)^2 - \rho^{-1}(2\,\nabla\rho\cdot\nabla\phi + \beta\nabla^2\rho). \tag{18}$$

Assuming that ρ is stationary $(\partial\rho/\partial t = 0)$ and eliminating ρ^2 between Eqs. (17) and (18), we obtain

$$\frac{\partial \phi}{\partial t} = -\omega(r) + \sigma_0 + \chi\nabla^2\phi + \sigma_0^{-1}\Lambda(\nabla\phi)^2 + 2\chi\rho^{-1}\,\nabla\rho\cdot\nabla\phi - \sigma_0^{-1}\Lambda\rho^{-1}\nabla^2\rho, \tag{19}$$

where $\sigma_0 = -\alpha$, $\chi = 1+\alpha\beta$, and $\Lambda = \alpha(\beta-\alpha)$. After applying the Hopf-Cole transformation

$$\phi = \sigma_0\Lambda^{-1}\chi(\ln Q - \ln\rho)$$

to Eq. (19), we find a new equation that Q should obey,

$$\frac{\partial Q}{\partial t} = \chi[\Lambda\chi^{-2} + \nabla^2 - (1+p^2)\rho^{-1}\nabla_r^2\rho]Q - p\omega(r)Q, \tag{20}$$

where $p = \chi^{-1}\sigma_0^{-1}\Lambda$. If the solution has rotational symmetry (e.g., the spiral wave solution), Q must be of the form [18]

$$Q(r,\theta,t) = q(r)e^{[p(\pm\theta-\Omega t)]}. \tag{21}$$

This expression is substituted into Eq. (20) to give an eigenvalue problem

$$\lambda q(r) = \hat{H}q(r) \tag{22}$$

in which

$$\lambda = -\chi^{-2}\Lambda(\sigma_0^{-1}\Omega + 1), \quad \hat{H} = \nabla_r^2 - [U(r) + \Delta U(r)],$$

$$U(r) = -p^2r^{-2} + (1+p^2)\rho^{-1}\nabla_r^2\rho,$$

$$\Delta U(r) = \begin{cases} 0 & \text{for } r > R, \\ \Delta U & \text{for } r \le R, \end{cases}$$

where $\Delta U = \chi^{-2}\sigma_0^{-1}\Lambda\Delta\omega$. While Eq. (22) is generally difficult to solve, it is still possible to give some discussion about what the equation implies. First, it clearly shows that the inhomogeneity modifies the potential $U(r) \to U(r) + \Delta U(r)$. This modification changes $\hat{H}$ and it turns out to affect the eigenvalue related to Ω and thus k via the dispersion relation. In other words, due to the existence of $\Delta U(r)$, the spatial distribution function $q(r)$ varies in two adjacent regions. Second, the sign of ΔU may be extremely important for pattern formation since it will locally increase $(\Delta U > 0)$ or decrease $(\Delta U < 0)$ the potential. In the framework of the phase dynamics approximation [18,19], it has been shown that the center region acts as a wave source if $\Delta U < 0$ and a wave sink if $\Delta U > 0$. Our numerical findings suggest that a necessary condition for sinklike spiral formation is $\Delta U > 0$ $[(\beta-\alpha)\Delta\omega < 0]$, which means the region enclosing the spiral center acts as a wave sink; for dense-sparse spiral patterns we find $\Delta U < 0$ $[(\beta-\alpha)\Delta\omega > 0]$, which describes the center region as a wave source.

Understanding the formation of dense-sparse spiral waves may turn out to shed light on the formation of sinklike spiral waves; so let us first consider the former structure with the parameters $\alpha = -0.5$ and $\beta = -1.4$ and $\Delta\omega = -0.2$, which indicates $(\beta-\alpha)\Delta\omega > 0$ and $\Delta U < 0$. In these circumstances, the core region $(r \le R)$ represents a wave source and from the uniform initial conditions an extended target pattern will be created [18,19]. To be precise, in contrast to the traveling wave patterns in the outside region $(r > R)$, a uniform oscillation occurs inside the core region, where no waves are observed. This target pattern is encountered frequently in nature, experiments, and simulations. If there is initially a spiral in the core region, we expect that it is possible to maintain its original rotating behavior since the core region exhibits self-oscillation. Due to the difference of the bulk frequency in the two neighboring regions, however, a self-modulation of the initial spiral must be observed. According to Fig. 5(a), one can see that the asymptotic frequency Ω_{k1} linearly depends on $\Delta\omega$ [$\Delta\omega < 0$ or $\Delta\omega > 0$ in Fig. 5(c)], which implies that the whole system is entrained by the core region. It is hence safe to say that wave-mediated synchronization of the adjacent region is guaranteed, which means $\Omega_{k1} = \Omega_{k2}$. With the help of dispersion relation (5), it is easy to find the relation of the wave numbers in two regions,

$$|k_1| - |k_2| = -\frac{\Delta\omega}{\beta-\alpha}(|k_1| + |k_2|)^{-1}, \tag{23}$$

where k_1 and k_2 denote the asymptotic wave numbers in the inner $(r \le R)$ and outer $(r > R)$ regions, respectively. Equation (23) clearly shows that, if $(\beta-\alpha)\Delta\omega > 0$, i.e., the heterogeneity acts as a wave source, the absolute wave number $|k_1|$ is always smaller than the one $|k_2|$ in the other region $(r > R)$. In this respect, we will observe a spiral structure

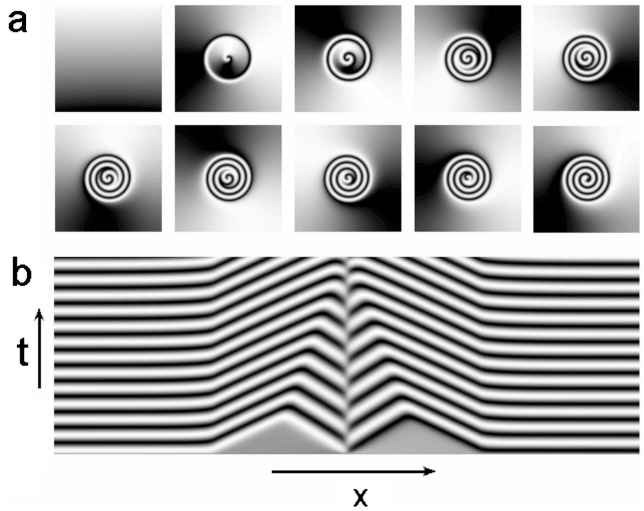

FIG. 7. Competition between spiral waves in the interior region and rotating waves in the outside region. (a) Snapshots for sinklike spiral pattern formation. The time interval between snapshots is unequal. (b) A partial space-time plot for (a) ($0 \le t \le 800$). The parameters are $\alpha=-0.10$, $\beta=-1.4$, $\Delta\omega=0.10$, and $R=90$. It is found that one type of wave is initially in the center region and the other is close to the interface, driven by the rotating waves in the outside region. It shows that the former is eventually suppressed by the latter.

with sparse arms in the core region and dense arms in the outside region as illustrated in Fig. 3(a).

Consequently, it is expected that, compared to the outside region, the spiral arms in the core region are denser if $(\beta-\alpha)\Delta\omega<0$; see Figs. 1(b) and 3(b). Considering $|k_1|^2 \gg |k_2|^2$ for the sinklike spiral, Eq. (23) can be further reduced as

$$|k_1|^2 = -\frac{\Delta\omega}{\beta-\alpha}. \tag{24}$$

In Figs. 5(b) and 5(d), we compare the numerical result (squares, solid line) with the theoretical predication (triangles solid line) via Eq. (24). Reasonable agreement is found. The interpretation of the possible mechanism underlying the formation of sinklike spiral structures can be made quite analogously with the discussions above for dense-sparse spiral waves. In the case of sinklike spiral pattern formation, if the initial condition is uniform, visible traveling waves will be able to emerge in the core region. However, the case may be remarkably changed when an initial spiral is put in the center region because of the competition between waves generated by the initial spiral center and by the rotating waves in the outside region. This viewpoint will become very clear provided that we adopt a cross-gradient initial condition rather than a well-developed spiral like Fig. 1(a). Figure 7 shows the competition between these two kinds of waves. Initially, there are two different waves appearing in the center region and close to the interface, respectively. As time elapses, waves generated by the initial spiral center are gradually taken over by rotating waves in the outside region. Numerical findings also demonstrate that the frequency of the sinklike spiral waves formed is smaller (greater) than that of spiral waves when $\Delta\omega$ is introduced in the whole medium (i.e., $R=\infty$) for $\beta-\alpha<0$ ($\beta-\alpha>0$) [see Figs. 5(a) and 5(c)]. This competition rule is the same as the case where a competition among two or more spirals takes place [16,36].

V. SINKLIKE SPIRAL WAVES IN THE OREGONATOR MODEL

To show that our observed results are robust and could be realized experimentally, numerical experiments are also performed on the Oregonator model, which is regarded as a good candidate for describing the light-sensitive BZ reaction. Recently, a recipe resulting in small-amplitude oscillation in a gel has been provided in Ref. [23]. This makes it possible to study the light response to the BZ reaction close to the Hopf bifurcation. Our numerical experiments are done with the reduced two component Oregonator model with oscillatory properties [48,49],

$$\frac{\partial u}{\partial t} = \frac{1}{\epsilon}\left(u - u^2 - [fv + \Phi(r)]\frac{u-q}{u+q}\right) + D_u\nabla^2 u,$$

$$\frac{\partial v}{\partial t} = u - v + D_v\nabla^2 v, \tag{25}$$

where u and v represent the concentrations of the autocatalytic species $HBrO_2$ and the catalyst, respectively. The parameter ϵ, similar to the one appearing in the FHN model, describes different reaction rates or time scales for the two species u and v; f and q are two other parameters. The effect of light on this reaction can be described by the additional term $\Phi(r)$ adopted in our simulations in the following form:

$$\Phi(r) = \begin{cases} \Phi_0 & \text{for } r > R, \\ \Phi_0 + \Delta\Phi & \text{for } r \le R. \end{cases} \tag{26}$$

Φ_0 denotes the background light intensity and the difference between the two subregions is reflected by $\Delta\Phi$. It is generally true that the frequency of chemical waves will be shifted as the light is switched on [50,51]; for the oscillatory light-sensitive BZ reaction, target patterns can be generated by nonuniform illumination, which has been experimentally studied in Ref. [22]. In our numerical case for the specific form of $\Phi(r)$ as Eq. (26), the center region plays the role of a wave source if $\Delta\Phi<0$ and a wave sink if $\Delta\Phi>0$.

According to the above discussions on sinklike spiral formation in the CGLE and the FHN model, we may predict that the sinklike spiral (dense-sparse spiral) can occur if $\Delta\Phi>0$ ($\Delta\Phi<0$) since the center region represents a wave sink (wave source). Numerical experiments indeed confirm this prediction; see Figs. 8(a) and 8(b). To be more precise, sinklike spiral waves are able to form when the center region is illuminated. The process of this kind of formation is almost the same as in the CGLE and the FHN model.

The examples of sinklike spiral waves so far discussed, in the CGLE, Fitzhugh-Nagumo, and Oregonator models, are limited to the sets of parameters that are in the vicinity of the Hopf bifurcation point. With these sets of parameters, the system exhibits sinusoidal oscillation with relatively small

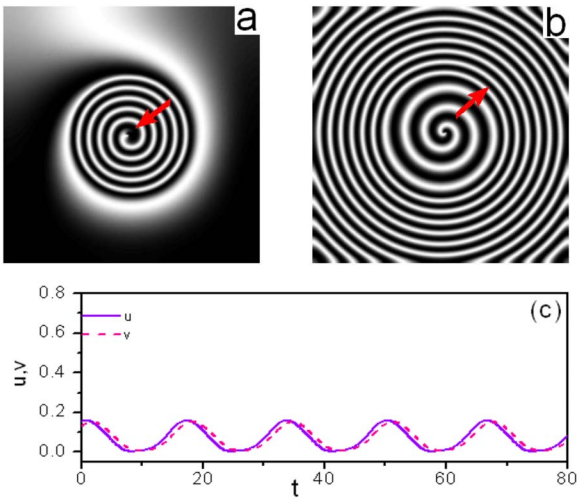

FIG. 8. (Color online) Sinklike and dense-sparse spiral patterns mediated by nonuniform light intensity in the Oregonator model. (a) $\Phi_0=0.0001$, $\Delta\Phi=0.000\,08$, sinklike spiral. (b) $\Phi_0=0.0001$, $\Delta\Phi=-0.000\,05$, dense-sparse spiral. (c) Time history of the activator u and the inhibitor v of the Oregonator model. It shows that the system exhibits small-amplitude nearly sinusoidal oscillations. The other parameters are $\epsilon=0.75$, $q=0.002$, $f=0.95$, $D_u=0.001$, $D_v=0.0001$, and $R=60$. The red arrow denotes the direction of the group velocity. Numerical simulations are performed on 256×256 grid points employing the explicit Euler method. The space and time steps are $\Delta x=\Delta y=0.5$ and $\Delta t=0.01$, respectively. No-flux conditions are imposed at the boundaries. The initial condition is a cross-gradient value of u and v.

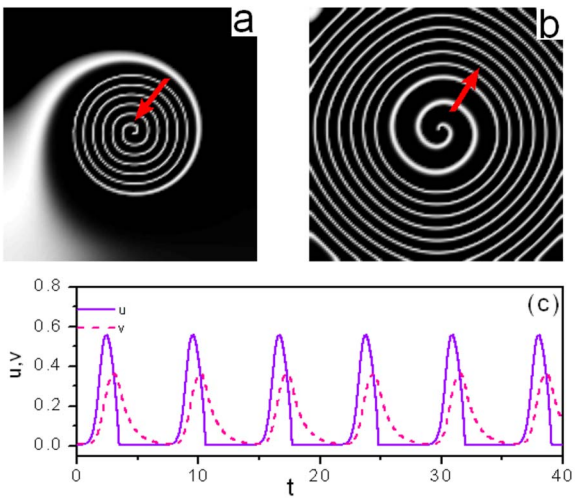

FIG. 9. (Color online) Sinklike and dense-sparse spiral patterns mediated by nonuniform light intensity in the Oregonator model, far from the Hopf bifurcation point. (a) $\Phi_0=0.000\,01$, $\Delta\Phi=0.0002$, sinklike spiral. (b) $\Phi_0=0.000\,11$, $\Delta\Phi=-0.0001$, dense-sparse spiral. (c) Time history of the activator u and the inhibitor v of the Oregonator model. It shows that the system exhibits anharmonic relaxation oscillation. The other parameters are $\epsilon=0.20$, $q=0.002$, $f=0.95$, $D_u=0.001$, $D_v=0.001$, and $R=30$. The red arrow denotes the direction of the group velocity. Numerical simulations are performed on 128×128 grid points employing the explicit Euler method. The space and time steps are $\Delta x=\Delta y=0.5$ and $\Delta t=0.002$, respectively. No-flux conditions are imposed at the boundaries. The initial condition is a cross-gradient value of u and v.

amplitude [see Fig. 8(c)]. Actually, a sinklike spiral wave is able to emerge even when the system is driven far way from the Hopf bifurcation point (in other words, the system exhibits relaxation oscillation). To show this point, we adopt another set of parameters with small ϵ (e.g., $\epsilon=0.2$) with typical relaxation oscillations [see Fig. 9(c)]. In this situation, sinklike and dense-sparse spiral waves sustained by nonuniform light intensity arise, as shown in Figs. 9(a) and 9(b). These numerical experiments again imply that the results presented here are quite robust and might be observed in experiments, such as the light-sensitive BZ reaction.

VI. CONCLUSION

We have examined spiral wave propagation in oscillatory systems with a disk-shaped inhomogeneity. Depending strongly on the properties of the medium and inhomogeneity, spiral waves can exhibit distinct behavior. For instance, an interesting spiral pattern called a sinklike spiral can emerge when the region enclosing the spiral center acts as a wave sink. In addition to sinklike spiral waves, other spiral patterns can also emerge. The possible mechanism underlying their formation is discussed based on the view of the inhomogeneity being a wave source or sink. In particular, we argue that the formation of the sinklike spiral is the result of the competition between the initial spiral waves in the center and rotating waves in the outside region. Further numerical simulations performed with various models such as the FHN and Oregonator models indicate that formation of sinklike spiral patterns is common and robust in nonuniform oscillatory media, where the circular interior region encloses the spiral tip.

The sinklike spiral found in this paper is worth mentioning because it differs considerably from previously found spiral waves such as NSs and ASs in the group velocity. For both NSs and ASs, the direction of the group velocity is away from the spiral center; while for sinklike spiral waves, it points toward the center. On the other hand, our findings strongly suggest that the effect of the inhomogeneity should not be neglected and in some cases even a weak inhomogeneity is capable of inducing remarkable effects. Finally, we hope our results will be realized in experiments, which would make our results more interesting from a practical point of view.

ACKNOWLEDGMENTS

We would like to thank Xiaoyi He for valuable discussions. This work was supported by the National Natural Science Foundation of China.

[1] A. T. Winfree, *The Geometry of Biological Time* (Springer, New York, 2001).
[2] J. D. Murray, *Mathematical Biology* (Springer, New York, 1999).
[3] A. T. Winfree, Science **175**, 634 (1972).
[4] Q. Ouyang and J.-M. Flesselles, Nature (London) **379**, 143 (1996).
[5] V. K. Vanag and I. R. Epstein, Science **294**, 835 (2001).
[6] S. Jakubith, H. H. Rotermund, W. Engel, A. von Oertzen, and G. Ertl, Phys. Rev. Lett. **65**, 3013 (1990).
[7] E. Palsson and E. C. Cox, Proc. Natl. Acad. Sci. U.S.A. **93**, 1151 (1996).
[8] J. M. Davidenko, A. V. Pertsov, R. Salomonsz, W. Baxter, and J. Jalife, Nature (London) **355**, 349 (1992).
[9] R. A. Gray, A. M. Pertsov, and J. Jalife, Nature (London) **392**, 75 (1998).
[10] S. Alonso, F. Sagués, and A. S. Mikhailov, Science **299**, 1722 (2003).
[11] H. Zhang, Z. Cao, N. J. Wu, H. P. Ying, and G. Hu, Phys. Rev. Lett. **94**, 188301 (2005); Z. Cao, P. Li, H. Zhang, F. Xie, and G. Hu, Chaos **17**, 015107 (2007).
[12] X. Zou, H. Levine, and D. A. Kessler, Phys. Rev. E **47**, R800 (1993).
[13] D. Pazo, L. Kramer, A. Pumir, S. Kanani, I. Efimov, and V. Krinsky, Phys. Rev. Lett. **93**, 168303 (2004).
[14] Y. Q. Fu, H. Zhang, Z. Cao, B. Zheng, and G. Hu, Phys. Rev. E **72**, 046206 (2005).
[15] A. M. Zhabotinsky, M. D. Eager, and I. R. Epstein, Phys. Rev. Lett. **71**, 1526 (1993).
[16] M. Hendrey, E. Ott, and T. M. Antonsen, Jr., Phys. Rev. Lett. **82**, 859 (1999).
[17] A. N. Zaikin and A. M. Zhabotinsky, Nature (London) **225**, 535 (1970).
[18] Y. Kuramoto, *Chemical Oscillation, Waves, and Turbulence* (Springer, Berlin, 1984).
[19] M. Stich and A. S. Mikhailov, Physica D **215**, 38 (2006).
[20] M. Jiang, X. Wang, Q. Ouyang, and H. Zhang, Phys. Rev. E **69**, 056202 (2004).
[21] X. He, H. Zhang, B. Hu, Z. Cao, B. Zheng, and G. Hu, New J. Phys. **9**, 66 (2007).
[22] H. Nagashima, J. Phys. Soc. Jpn. **60**, 2797 (1991).
[23] H. Skodt and P. G. Sorensen, Phys. Rev. E **68**, 020902(R) (2003).
[24] J. Maselko and K. Showalter, Nature (London) **339**, 609 (1989).
[25] J. Davidsen, L. Glass, and R. Kapral, Phys. Rev. E **70**, 056203 (2004).
[26] M. Bär, I. G. Kevrekidis, H.-H. Rotermund, and G. Ertl, Phys. Rev. E **52**, R5739 (1995).
[27] A. P. Munuzuri, V. A. Davydov, M. Gomez-Gesteira, V. Perez-Munuzuri, and V. Perez-Villar, Phys. Rev. E **54**, R5921 (1996).
[28] J. Sainhas and R. Dilao, Phys. Rev. Lett. **80**, 5216 (1998).
[29] F. Xie, Z. Qu, J. N. Weiss, and A. Garfinkel, Phys. Rev. E **63**, 031905 (2001); F. Xie and J. N. Weiss, *ibid.* **75**, 016107 (2007).
[30] M. Gutman, I. Aviram, and A. Rabinovitch, Phys. Rev. E **69**, 016211 (2004).
[31] M. Zhan, X. Wang, X. Gong, and C.-H. Lai, Phys. Rev. E **71**, 036212 (2005).
[32] Z. Cao, H. Zhang, and G. Hu, Europhys. Lett. **79**, 34002 (2007).
[33] R. Zhang, L. Yang, A. M. Zhabotinsky, and I. R. Epstein, Phys. Rev. E **76**, 016201 (2007).
[34] H. Kitahata and K. Yoshikawa, J. Phys.: Condens. Matter **17**, S4239 (2005).
[35] H. Kitahata, A. Yamada, S. Nakata, and T. Ichino, J. Phys. Chem. A **109**, 4973 (2005); S. Nakata, S. Morishima, and H. Kitahata, *ibid.* **110**, 3633 (2006); S. Nakata, S. Morishima, T. Takatoshi, and H. Kitahata, *ibid.* **110**, 13475 (2006).
[36] L. B. Smolka, B. Marts, and A. L. Lin, Phys. Rev. E **72**, 056205 (2005).
[37] M. Ipsen, L. Kramer, and P. G. Sorensen, Phys. Rep. **337**, 193 (2000).
[38] I. S. Aranson and L. Kramer, Rev. Mod. Phys. **74**, 99 (2002).
[39] M. C. Cross and P. C. Hohenberg, Rev. Mod. Phys. **65**, 851 (1993).
[40] P. S. Hagan, SIAM J. Appl. Math. **42**, 762 (1982).
[41] E. M. Nicola, L. Brusch, and M. Bär, J. Phys. Chem. B **108**, 14733 (2004).
[42] L. Brusch, E. M. Nicola, and M. Bär, Phys. Rev. Lett. **92**, 089801 (2004).
[43] Y. F. Gong and D. J. Christini, Phys. Rev. Lett. **90**, 088302 (2003).
[44] V. N. Biktashev, Phys. Rev. Lett. **95**, 084501 (2005).
[45] C. Wang, C. X. Zhang, and Q. Ouyang, Phys. Rev. E **74**, 036208 (2006).
[46] O. A. Mornev, I. M. Tsyganov, O. V. Aslanidi, and M. A. Tsyganov, JETP Lett. **77**, 270 (2003).
[47] R. FitzHugh, Biophysics (Oxf.) **1**, 445 (1961); J. S. Nagumo, S. Arimoto, and S. Yoshizawa, Proc. IRE **50**, 2061 (1962).
[48] R. J. Field, E. Koros, and R. M. Noyes, J. Am. Chem. Soc. **94**, 8649 (1972).
[49] J. J. Tyson and P. C. Fife, J. Chem. Phys. **73**, 2224 (1980).
[50] V. Petrov, Q. Ouyang, G. Li, and H. L. Swinney, J. Phys. Chem. **100**, 18992 (1996).
[51] A. Belmonte and J.-M. Flesselles, Phys. Rev. Lett. **77**, 1174 (1996).